Available online at www.sciencedirect.com

ScienceDirect

Procedia Engineering 191 (2017) 1096 – 1103

Procedia Engineering

www.elsevier.com/locate/procedia

Symposium of the International Society for Rock Mechanics

Simulating the Single- and Multi-Stage Hydraulic Fracturing: Some Insights Gleaned from Discontinuum and Continuum Modelling

H. Konietzky*, P.L.P. Wasantha, F. Weber

Geotechnical Institute, TU Bergakademie Freiberg, Gustav-Zeuner-Str. 1, 09596 Freiberg, Germany

Abstract

Discontinuum and continuum modelling approaches were used to simulate the single- and multi-stage hydraulic fracturing. Two-dimensional discontinuum modelling of single-stage fracturing revealed a marked modification of the stress field in the vicinity of the fracture (stress shadow effect) during fracture propagation which was identified as the reason for the significant asymmetry of fracture propagation about the wellbore observed for multi-stage fracturing. Allowing the fracturing fluid to flow back after each fracturing stage appeared to minimize this stress shadow effect on fracture propagation geometry. Three-dimensional discontinuum modelling results showed similar behaviors as two-dimensional modelling. Inclined orientation of wellbores with respect to principal stresses and enabling fluid backflow after each fracturing stage were found to be effective to minimize the stress shadow effect on fracture propagation geometry after three-dimensional discontinuum modelling. Our three-dimensional continuum modelling of hydraulic fracture propagation so far revealed some promising results demonstrating its capability to simulate hydraulic fracturing applications. Finally, the specific and contrasting features of both approaches are discussed here giving some useful insights into both approaches to assist users with choosing the appropriate method for a particular simulation project.

Peer-review under responsibility of the organizing committee of EUROCK 2017

Keywords: Hydraulic fracturing; Discontinuum modelling; Continuum modelling

1. Introduction

Hydraulic fracture stimulation involves complex interactions of many processes and parameters, and understanding their independent and coupled roles on the overall treatment process is imperative for improved

* Corresponding author. Tel.: +493731-39-2519; fax: +493731-39-3638.
E-mail address: Heinz.Konietzky@ifgt.tu-freiberg.de

1877-7058
Peer-review under responsibility of the organizing committee of EUROCK 2017
doi:10.1016/j.proeng.2017.05.283

productivity. In-situ stress state, thermo-hydro-mechanical properties of the reservoir rock, the presence and properties of natural fractures, and operational parameters such as injection rate and the properties of fracturing fluid are of significant influence on the hydraulic fracture stimulation process, among others [1–3].

Issues such as the cost, time and intensive labor have severely curbed the possibility of performing a series of experiments with representatively large specimens to explore the hydraulic fracture propagation behavior under different reservoir conditions. Thus, numerical simulation has been the preferred technique to understand the various underlying mechanisms of hydraulic fracture propagation under reservoir conditions [4]. Both discontinuum and continuum approaches are available for hydraulic fracturing simulations with their intrinsic pros and cons. Therefore, one must be cognizant of the limitations and specific capabilities of these different approaches to select the most appropriate method for a particular design or investigation. We summarize here the results of a comprehensive study that used discontinuum modelling to explore the single and multi-stage hydraulic fracture propagation under reservoir conditions as well as the preliminary verification results of continuum-based hydraulic fracturing simulations.

2. Discontinuum modelling approach

Discontinuum approach is a relatively new but widely-using technique in rock mechanics and rock engineering. This approach emphasizes on the blocky nature of a system where neighboring blocks interact through their interfaces (i.e. joints). The blocks can be made rigid or deformable and both two-dimensional (2D) and three-dimensional (3D) analyses are presently possible with discontinuum modelling. We selected universal distinct element code (UDEC) and three-dimensional distinct element code (3DEC) software for 2D and 3D simulations, respectively.

For the discontinuum-based simulations here (both 2D and 3D), the region of Freiberg (Saxony, Germany), which is a potential location for a geothermal power plant [5], is used as a case example. The target reservoir is a granite intrusion occurs within a depth between four and five kilometers, which is overlaid by Gneiss. The in-situ stress field of the target region has been determined and the principal stresses demonstrate a significant contrast [5]. Experimentally determined properties of these granite and gneiss rocks are summarized in Table 1.

Table 1. Geo-mechanical properties of Granite and Gneiss from Freiberg area (after [5]).

Parameter	Granite	Gneiss
Density [$kg \cdot m^{-3}$]	2660	2700
Young's Modulus [GPa]	65.0	55.0
Poisson's ratio [-]	0.22	0.30
Tensile strength [MPa]	9.0	9.0
Cohesion [MPa]	3.8	3.1
Friction angle [°]	40.8	35.5

2.1. Two-dimensional analysis

Both single- and multi-stage fracturing were simulated using UDEC. A 2000m x 2000m model was first created for which major and minor principal stresses (160 and 80 MPa, respectively) were applied on vertical and horizontal boundaries, respectively (Figure 1a). A pre-defined joint oriented normal to the minor principal stress direction was embedded in the model for hydraulic fracture propagation as the blocks are indivisible (more of such joints were embedded for multi-stage fracturing). A fluid having properties akin to those of water at room temperature was injected at a rate of 0.0833 $m^3 \cdot s^{-1}$ to the domain nearest to the center of the embedded joint at each fracturing stage.

Fracture length, width (a_h) and the distribution of the change of minor principal stress ($\Delta\sigma_3$) at the end of single-stage fracturing simulation are shown in Figure 1b. Fracture length of 295m with an average aperture of 2.6 cm and a maximum aperture of 3.3 cm at the injection point can be observed from Figure 1b. In addition, Figure 1b shows a significant modification of the minor principal stress field in the vicinity of the hydraulic fracture. The regions above and below the fracture show an increase of σ_3 indicating a marked stress shadow effect whereas the σ_3 at the fracture front is relatively lower.

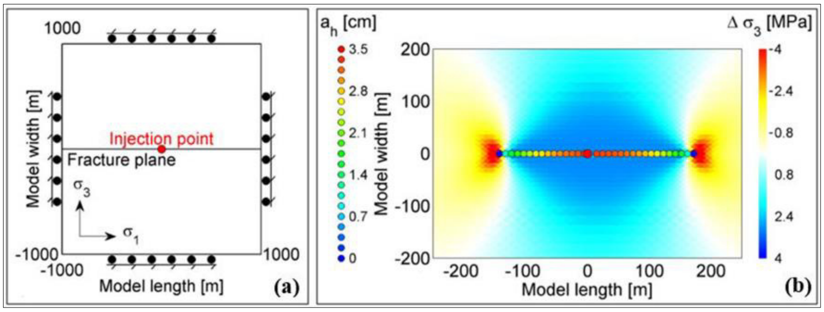

Fig. 1. (a) 2D model arrangement; (b) fracture aperture a_h, length, and minor principal stress change $\Delta\sigma_3$ distribution after the simulation.

Multi-stage fracturing was then simulated for which five fracturing stages with wellbores spaced by 50 m were considered. Fluid was sequentially injected (from top to bottom in Figure 2) to the five wellbores for 100 seconds for each well. Figure 2a shows the fracture geometries and $\Delta\sigma_3$ distribution within the model after completing the simulation. The fracture length in Figure 2a indicates a marked asymmetry about the wellbore which is undesirable for the economics of the project. After the first well stimulation subsequent stimulations show a directional bias of fracture propagation dictated by the changes of minor principal stress distribution. In other words, the development of stress shadow during one fracturing stage influences the fracture propagation of subsequent fracturing stage. Parting the wellbores further can minimize the effect of stress shadow, but it can be unfavorable for the project economics.

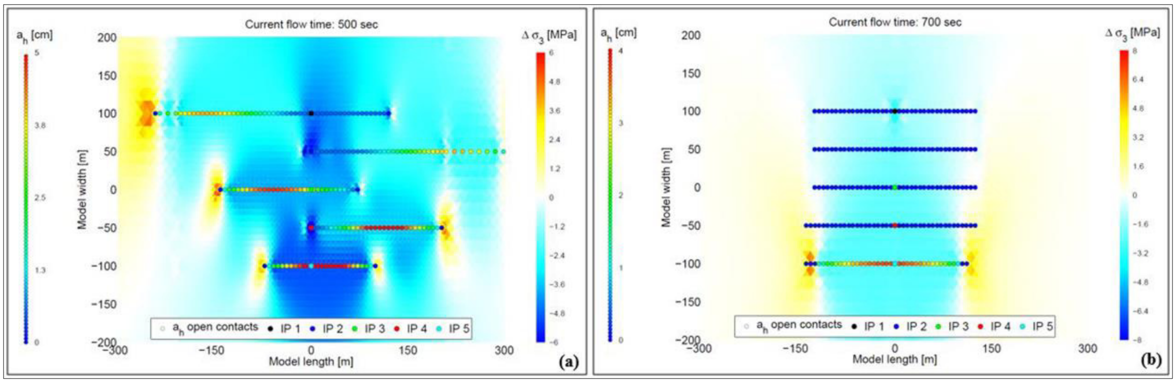

Fig. 2. Fracture aperture a_h, length, and minor principal stress change $\Delta\sigma_3$ distribution after multi-stage fracturing simulation (a) without fluid backflow; (b) with fluid backflow.

We then simulated the scenario of multi-stage fracturing with enabled backflow of the injected fluid after each fracturing stage. The fracture geometries and the distribution of $\Delta\sigma_3$ within the model for this case are shown in Figure 2b. It can be seen that the fracture propagation is more or less symmetrical about the wellbore for each fracturing stage. Anomalies of the stress field can be greatly eased off and stresses can be stabilized to some extent by allowing the fluid to flow back after fracturing. Therefore, the stress shadow effect becomes less pronounced compared to the previous case, where no fluid back flow was allowed, leading to a closely symmetrical fracture propagation.

2.2. Three-dimensional analysis

Modelling with 3DEC allows studying the hydraulic fracture propagation under the three-dimensional in-situ stress state. Similar to UDEC, fluid flow is allowed only along predefined fracture planes. We conducted both single and multi-stage simulations and the model set-ups for both cases are shown in Figure 3.

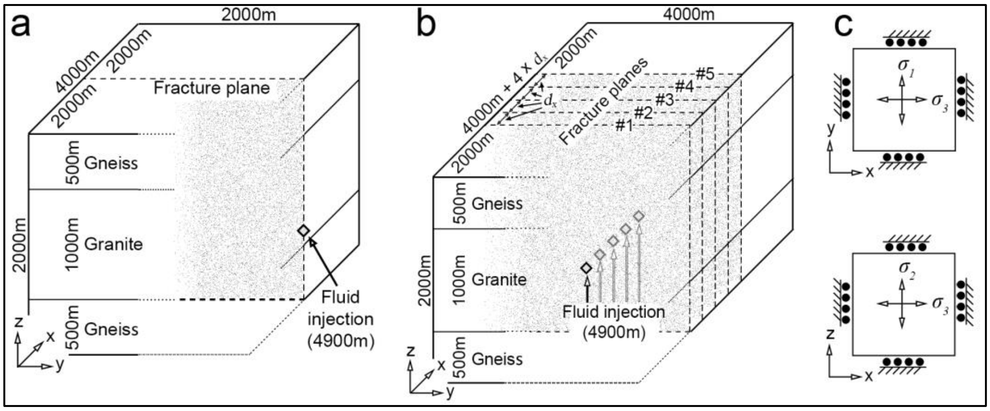

Fig. 3. (a) Model set-up for single-stage fracturing (one half of the fracture); (b) model set-up for multi-stage fracturing; (c) orientation of the principal stress components for simulations (modified after Zeeb and Konietzky [6]).

Figure 4a displays the fracture height and aperture growth characteristics for single-stage fracturing (note that only one half the problem domain was simulated and the fracture geometry of that half was mirrored to obtain the geometry of the complete fracture). It can be seen from Figure 4a that the hydraulic fracture is predominantly propagating vertically upwards from the wellbore location as a result of the gradual decrease of the stress along the upward vertical direction (i.e. the overburden stress). In addition, Figure 4a shows that greater fracture apertures are located in the upper part of the fracture as a product of the higher normal stress acting on the lower portion of the fracture. Figure 4b is a 3D representation of the fracture geometry and the distribution of $\Delta\sigma_3$ within the surrounding of the fracture. A clear stress shadow effect is apparent from Figure 4b where a greater stress accumulation parallel to the fracture and relatively lower stress in the fracture forefront can be observed.

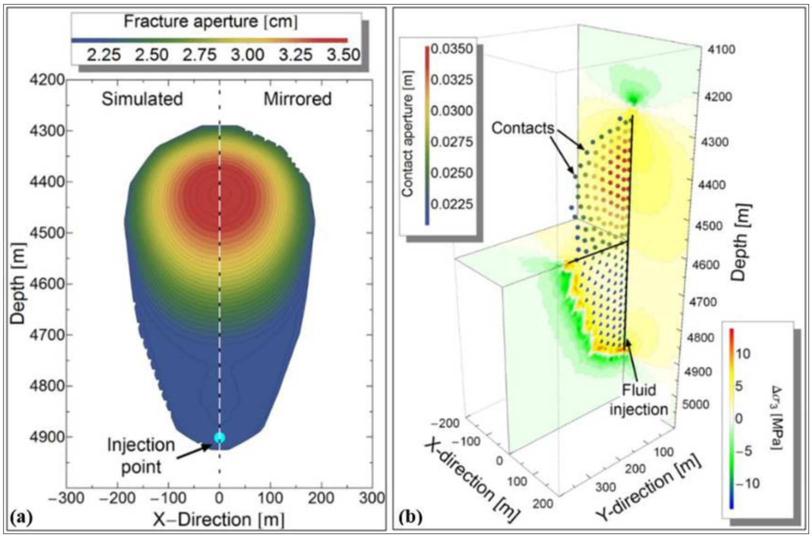

Fig. 4. (a) Geometry of the fracture after single-stage fracturing; (b) 3D illustration of the fracture geometry and minor principal stress change $\Delta\sigma_3$ distribution after single-stage fracturing.

Multi-stage fracturing with five sequential stages was then simulated with the wellbore arrangement similar to Figure 3b (spacing between wellbores was 100 m). Three-dimensional fracture profiles along with the fracture apertures after completing the simulation are shown in Figure 5a. As in the case of single-stage fracturing all fractures have predominantly propagated vertically upward due to the vertical stress gradient effect and greater fracture apertures are located in the upper portion of the fractures. However, a significant deflection of fractures from the vertical plane through the wellbores can be observed from Figure 5a. This was identified as a product of the stress shadow effect as in the case of 2D multi-stage simulations. In other words, changes of the minor principal stress field after one fracture stimulation influence the fracture propagation of subsequent stimulations. Unsystematic fracture propagation in this manner is detrimental for economic production.

We then considered a case where wellbores are placed diagonally in the horizontal plane (X-Y plane) which means that they are oriented at an angle of 45° with the X-direction (and Y-direction). Fluid backflow after each stimulation stage was allowed and the distance between two wellbores was set as 200 m. The fracture profiles after completing all the stimulations are shown in Figure 5b. As can be seen from Figure 5b, fractures still propagate with the preferred vertically upward direction (Fracture #5 is an exception which propagated into a part of the model with coarser meshing). The highest change of minor principal stress, which was determined as ±12 MPa for the previous case, is now ±7 MPa and indicates a less influence of stress shadow in the modified model arrangement. While completely avoiding the stress shadow effect and associated fracture deflection is difficult, we suggest that the modified wellbore arrangement proposed here is capable of minimizing its influence for multi-stage fracturing.

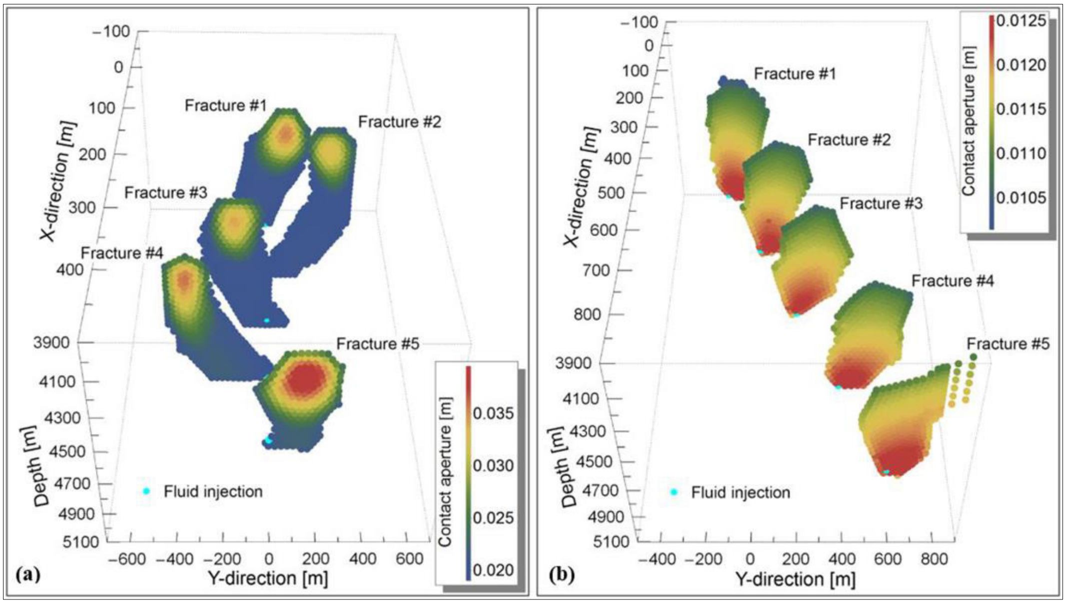

Fig. 5. 3D illustration of the locations of failed sub-contacts and fracture profiles for (a) original model set-up; (b) modified model set-up (modified after Zeeb and Konietzky [6]).

3. Continuum modelling approach

The continuum modelling approach is based on a macroscale concept where the rock material is unable to break across or to open at any point within the model domain [7]. Most popular continuum-based modelling methods are finite difference method (FDM), finite element method (FEM, XFEM) and boundary element method (BEM) [7]. In this study, the FDM code FLAC^{3D} is selected for continuum-based hydraulic fracturing simulation. The modelled rock is discretized into finite difference zones and grid points to replace the partial differential equations of motion by algebraic equations [8]. FLAC^{3D} offers fully hydro-mechanical coupling based on Biot's theory of porous media [9].

Since the continuum approach is not capable of modelling the fractures explicitly, the concept of virtual cracks, based on the work of Zhou et al. [10], is used to model hydraulic fracture propagation. In this concept, fractures are represented by failed zones where the fracture opening is expressed via grid point displacements. With the beginning of fluid injection pressure builds up within the injection area. If the rock in this area fails according to a prescribed constitutive law (Mohr-Coulomb constitutive law in this case) the fracture initiates and propagates under the existing stress state. Thus, the zones of the model are categorized into three types; fractured, partially-fractured and unfractured. Based on crack opening (grid point displacements), the fracture permeability of one zone increases according to the cubic law [11, 12]. Afterwards, a particular mean value between fracture and rock permeability is calculated for each zone. In contrary to Zhou et al. [10], the fractures in the models of present study propagate liberally within the model and not along predefined interfaces, which is a significant advantage and basis for modelling of even complex fracture systems.

The FLAC^{3D} algorithm for detailed investigations of hydraulic fracturing simulation is under development and here we present a verification example to demonstrate the feasibility of continuum approach for hydraulic fracturing simulation. Table 2 contains the numerical input parameters used for this verification model.

Table 2. Numerical input parameters for verification model.

Parameter	Granite
Density [$kg \cdot m^{-3}$]	2600
Bulk Modulus [GPa]	5.5
Shear Modulus [GPa]	4.17
Tensile strength [Pa]	0
Cohesion [MPa]	10.0
Friction angle [°]	10
Permeability [m^2]	9E-22
Porosity [-]	0.2
Injection rate [$m^3 \cdot s^{-1}$]	5E-3
Fluid Density [$kg \cdot m^{-3}$]	1000
Major, intermediate and minor principle stresses [MPa]	10.0, 7.0, 2.0

Figure 6 shows a schematic diagram of the developed model assuming symmetry about the bottom x-y plane and the x-z plane running through the fluid injection area. The model represents the upper left quarter of the complete problem domain.

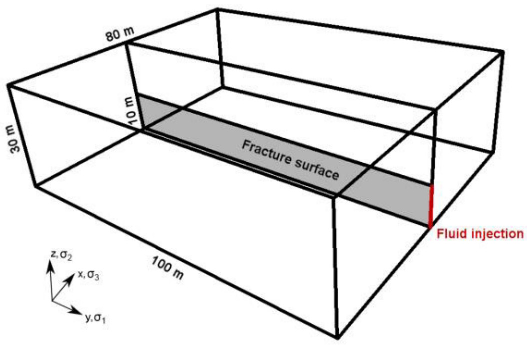

Fig. 6. Model geometry and the alignment of principal stresses for the verification model.

Roller boundary conditions were applied to all model faces. The analytical solution of Perkins-Kern-Nordgren (PKN) fracture model [13–15] is used here for the model verification. Hence, the half-height of the fracture is restricted to 10 m that fulfils PKN assumptions and fluid is injected over the whole fracture height. These arrangements force the vertical fracture to propagate horizontally. The rock material is assumed homogenous, isotropic and impermeable. Note that due to the nature of the alignment of principal stresses the fracture will propagate within the marked fracture surface of Figure 6 which is not predefined. After the model set-up simulation was continued until a 50 m long fracture is developed. Failed zones representing the fracture and the top view of the displacement vectors showing fracture opening are shown in Figure 7a and 7b, respectively. The fracture has propagated perpendicular to the minor principal stress from the area of fluid injection, according to Figure 7a. In addition, Figure 7b displays an elliptical fracture opening that agrees with PKN model assumptions.

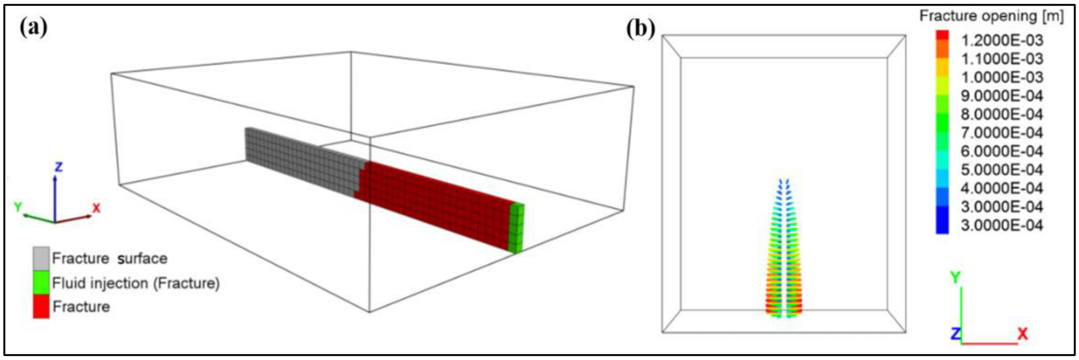

Fig. 7. (a) Propagated fracture profile after FLAC^{3D} simulation, and (b) top view of the displacement vectors of the fracture.

Figure 8 shows a compilation of different hydraulic parameters. The pressure distribution (Figure 8a) within the fracture is nearly uniform (2.4 to 2.6 MPa) which is consistent with the assumptions of PKN model. Variation of fracture opening (measured at the bottom x-y plane of the model) along the fracture length derived from the FLAC^{3D} model together with the corresponding variation of PKN analytical model (Figure 8c) shows a good consistency implying that the developed FLAC^{3D} model is capable of capturing key mechanics of hydraulic fracture propagation.

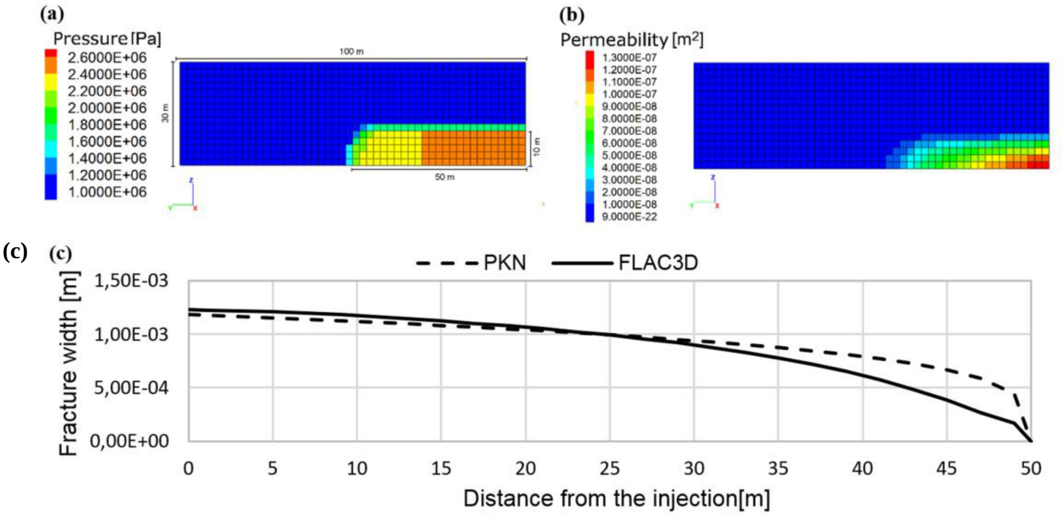

Fig. 8. Hydraulic parameter response of the verification model in FLAC^{3D}, (a) fluid pressure in the fracture and (b) fracture permeability along the cross section in the y-z plane, and (c) numerically and analytically calculated fracture width vs. distance from the injection point.

Permeability distribution within the fracture, determined using the calculated fracture width for each zone and following the cubic law [11], is shown in Figure 8b. Highest values of permeability can be observed at the middle of the fracture. Due to the elliptical nature of the fracture, permeability decreases with increasing distance from the injection area. Intact rock permeability remained constant throughout the calculations.

4. Summary and conclusions

Discontinuum and continuum modelling approaches were employed to simulate the single- and multi-stage hydraulic fracturing. One fundamental difference between the two approaches is the fracture initiation and propagation mechanism where discontinuum modelling uses predefined paths along block/particle boundaries for fracture propagation whereas fracture propagation is simulated by the smeared-zone concept in continuum modelling. Both modelling procedures can simulate tensile and shear fractures as well as mixed-mode fractures. We successfully used the two-dimensional numerical code, UDEC, and three dimensional numerical code, 3DEC (both are discontinuum-based), to comprehensively understand the hydraulic fracture propagation under reservoir conditions. The main highlight of the results of these simulations is the significant stress shadow effect that causes a marked asymmetry of fracture propagation about the wellbore. We present here some alternative techniques to minimize the stress shadow effect and consequently the asymmetry of the fracture propagation. Our preliminary verification modelling so far with continuum-based FLAC^{3D} has revealed some promising results for which we found a good consistency between our modelling results and those of a popular analytical model. Further modelling with FLAC^{3D} is currently underway and the results will be published later.

References

[1] N.R. Warpinski, L.W. Teufel, Influence of geologic discontinuities on hydraulic fracture propagation, J. Petrol. Technol. (1987) 209–220.
[2] P.L.P. Wasantha, H. Konietzky, Fault reactivation and reservoir modification during hydraulic stimulation of naturally-fractured reservoirs, J. Nat. Gas. Sci. Eng. 34 (2016) 908–916.
[3] C.E. Renshaw, D.D. Pollard, An experimentally verified criterion for propagation across unbonded frictional interfaces in brittle, linear elastic materials, Int. J. Rock Mech. Min. Sci. 32 (1995) 237–249.
[4] G. Preisig, E. Eberhardt, A. Hosseinian, M. Bustin, Coupled hydromechanical modeling of rock mass response to hydraulic fracturing: Outcomes related to the enhancement of fracture permeability, in: 13th International Congress of Rock Mechanics, 10-13 May, Montréal, Canada, 2015.
[5] LfULG (Landesamt für Umwelt, Landwirtschaft und Geologie), Tiefengeothermie Sachsen. Schriftenreihe Heft 9/2011; Freistaat Sachsen.
[6] C. Zeeb, H. Konietzky, Simulating the hydraulic stimulation of multiple fractures in an anisotropic stress field applying the discrete element method, Energy Procedia 76 (2015) 264–272.
[7] L. Jing, A review of techniques, advances and outstanding issues in numerical modelling for rock mechanics and rock engineering. International Journal of Rock Mechanics & Mining Sciences 40 (2003) 283–353.
[8] ITASCA, FLAC3D manual version 5.0, Itasca Consulting Group Inc., Minneapolis, USA, 2013.
[9] M.A. Biot, General theory of three-dimensional consolidation. Journal of Applied Physics, (1941), 155-164.
[10] L. Zhou, M.Z. Hou, A new numerical 3D-model for simulation of hydraulic fracturing in consideration of hydro-mechanical coupling effects, International Journal of Rock Mechanics & Mining Science 60 (2013) 370–380.
[11] D.T. Snow, A parallel plate model of fractured permeable media. PhD Thesis, University of California, Berkeley, USA, 1965.
[12] C. Louis, Strömungsvorgänge in klüftigen Medien und ihr Wirkung auf die Standsicherheit von Bauwerken und Böschungen im Fels [Flow phenomena in fractured systems and their contribution to structural integrity of buildings and slopes at rock], PhD Thesis Technical University Karlsruhe, Germany, 1967.
[13] T.K. Perkins, L.R. Kern, Widths of hydraulic fractures, Journal of Petroleum Technology (1961) 937–949.
[14] R.P. Nordgren, Propagation of a vertical hydraulic fracture, Society of Petroleum Engineers Journal (1972) 306–314.
[15] B.R. Meyer, Design formulae for 2-D and 3-D vertical hydraulic fractures: model comparison and parametric studies, SPE unconventional gas technology symposium of petroleum engineers Louisville 18-21 May, 1986, SPE 15240.